energies

MDPI

Article

The Saturated Water Content of Liquid Propane in Equilibrium with the sII Hydrate

Kayode I. Adeniyi, Connor E. Deering and Robert A. Marriott *

Department of Chemistry, University of Calgary, 2500 University Drive, NW, Calgary, AB T2N 1N4, Canada; kadeniyi@ucalgary.ca (K.I.A.); cedeerin@ucalgary.ca (C.E.D.)

* Correspondence: rob.marriott@ucalgary.ca

Received: 20 October 2020; Accepted: 26 November 2020; Published: 29 November 2020

Abstract: In order to prevent solids from forming during the transportation and handling of liquid propane, $C_3H_8(l)$, the fluid is dehydrated to a level below the water dew point concentration for the coldest operating temperature. Thus, accurate calculation of the saturation water content for C_3H_8 is important to determine the designed allowable concentration in liquid C_3H_8. In this work, we measured the water content of liquid C_3H_8 in the presence of the structure II hydrate from p = 1.081 to 40.064 MPa and T = 241.95 to 276.11 K using a tunable diode absorption spectroscopy technique. The water content results were modelled using the reference quality reduced Helmholtz equations and the Sloan et al. model for the non-hydrate and hydrate phases, respectively. Calculations show a good agreement (an average difference of less than 12 ppm) when compared to our measurements. Furthermore, the model was also used for calculating the dissociation temperatures for three phase loci, where a relative difference greater than 5 K was observed compared to the literature, hence our previously model reported by Adeniyi et al. is recommended for three phase loci calculations.

Keywords: propane; structure type II hydrate; water content; flow assurance

1. Introduction

In natural gas processing, natural gas liquids (NGL) are separated from methane by cooling down the natural gas stream to low temperatures in a cryogenic process [1]. The presence of water (H_2O) during this process is highly undesirable because it can cause the formation of solid clathrate hydrates which can restrict and compromise the performance of heat exchangers and expanders [2,3]. Clathrate hydrates are non-stoichiometric solids formed when water molecules forms cages that encapsulated appropriate sized molecules at the correct conditions, usually at low temperature and high pressure [3]. A common NGL is propane, $C_3H_8(l)$, which is sold as a fuel or chemical feedstock. C_3H_8 forms a relatively stable structure II hydrate (sII) which can be further stabilized by accommodating other structure I (sI) formers [4].

While the three phase (Lw-H-C_3H_8(g) and Lw-H-$C_3H_8(l)$) dissociation/formation conditions have been well studied in the literature [5–21], the two-phase $C_3H_8(l)$-hydrate system has not received the same attention, especially at higher pressure [22–25]. In a previous study, we reported the dissociation data along the three phase loci for C_3H_8, where the poor agreement along the Lw-H-$C_3H_8(l)$ was attributed to buoyancy and the lower density of C_3H_8 hydrate relative to the aqueous phase [21]. Accurate calculation of saturated hydrate dissociation conditions or water content of C_3H_8 is important, considering that a hydrate can also form without a liquid water phase or directly from dissolved water.

In this work, we measured the water content of liquid propane in equilibrium with a hydrate from p = 1.081 to 40.064 MPa and T = 241.95 to 276.11 K using a tunable diode absorption spectroscopy technique. The same technique was previously used for water content with liquid CO_2 and liquid H_2S sI formers [26,27]. In similar fashion, the results for the H-$C_3H_8(l)$ system were modeled using the

reduced Helmholtz energy equations-of-state (EOSs) of Wagner and Pruβ [28] and Lemmon et al. [29] together with the mixing model of Kunz and Wagner [30] for the non-hydrate phases, and the van der Waals and Platteuw [31] and Sloan et al. [22] equation for the hydrate phase. The fluid phase calculation was implemented within the REFPROP 10.0 software (Gaithersburg, MD, USA) [32]. Using the same optimised parameters, this model also was used to calculate the three-phase dissociation conditions. The calculations from the model were subsequently compared to experimental data and the differences are discussed in the latter sections.

2. Experimental Section

2.1. Materials

High purity C_3H_8 (99.999 mol%) was used for feed preparation in this work and was supplied by Linde Canada Ltd. The purity of the C_3H_8 fluid was confirmed with a Bruker 450-gas chromatograph chromatography equipped with a thermal conductivity detector and a flame ionization detector. The distilled water used was polished by an EMD Millipore model Milli-Q Type 1 water purification system (SigmaAldrich, Canada) to a resistivity of 18 MΩ·cm and degassed by stirring under vacuum for a minimum of 24 h.

2.2. Experimental Apparatus

The small equilibration loop, coupled with a tunable diode laser spectrometer (TDLAS), was used in this work and has been extensively described in a previous study [26]; however, a brief explanation is provided here. The setup consists of coiled SS316 tube (ca. 3 cm^3; 0.71 mm I.D.) which acts as a cold tube for a slow flowing saturated mixture of C_3H_8 + H_2O. A heated single-phase mixture is delivered to the tube using a Teledyne 260D ISCO syringe pump. In this work, room temperature, $T > 293$ K, was warm enough to hold the synthetic C_3H_8 + H_2O mixtures in the single phase.

The fluid exits the end of the tubing after reaching equilibrium with the hydrate using a 2-way on/off poppet valve (Valco Instruments Co. Inc.) to flash the saturated fluid to the TDLAS for water concentration measurement. A PolyScience PP07R-40 refrigerated bath circulating a 30:70 water-glycol mixture controls and regulates the temperature of the system to within ±0.004 K. The temperature of the system was measured using an ITS-90 calibrated four-wire platinum resistance thermometer (PRT) with an uncertainty better than 0.005 K [33], while the pressure is measured with a calibrated Keller Druckmesstechnik PA-33X transducer (δp = ± 0.001 MPa).

2.3. Experimental Procedure

The C_3H_8 + H_2O single-phase feed was prepared gravimetrically in a 500 cm^3 SS316 vessel on a Mettler–Toledo XP26003L comparator that has an accuracy of δm = ±1 mg. Prior to the transfer of feed to the syringe pump, the mixture was agitated for three weeks on a rocking table to allow for thorough mixing of the components. Before any measurement, the setup was evacuated for a minimum of 24 h using a vacuum of 2.5×10^{-7} MPa. The SS316 tubing was flushed with the feed sample prior to charging to a desired pressure via the ISCO syringe pump. The temperature of the coiled loop was first maintained at 298 K in order to check the TDLAS factory calibration with the known concentration, by periodically opening of the poppet valve for 145 ms every 30 s until the reading on the TDLAS stabilized to within a standard deviation of 4 ppmv. Following the calibration check procedure, the temperature of the system was then lowered to 238 K and maintained for at least four days to allow for hydrates to fully form. After this period, the equilibrated effluent was sampled to the TDLAS analyzer by periodically opening of the poppet valve for 145 ms every 60 s until the reading stabilized to within a standard deviation of 4 ppmv.

3. Description of the Thermodynamic Model

For two-phase equilibria involving a hydrate phase, the following criterion must be met:

$$f_i^H = f_i^b \text{ or } f_i^{aq} = f_i^b \tag{1}$$

where f_i is the fugacity of H_2O or C_3H_8 in the C_3H_8+hydrate system, the superscript H, aq, and b denote the hydrate phase, aqueous phase, and non-aqueous phase, respectively. Note that the lowest binary equilibria fugacities will be spontaneously favoured through Gibbs energy minimization; therefore, the smaller fugacity for the hydrate or aqueous phase will dictate which binary equilibrium is favoured.

For three phase equilibrium calculation, fugacities in all three phases will be equal:

$$f_i^H = f_i^{aq} = f_i^b, \tag{2}$$

3.1. Fluid Phase

The fugacities of $H_2O(l)$ and $C_3H_8(g\&l)$ were calculated using Wagner and Pruβ [28] and Lemmon et al. [29] EOSs, respectively. The fugacity of hexagonal ice was calculated using the Feistel and Wagner EOS [34]. The fluid equations were coupled with the mixing model of Kunz and Wagner [30] and are implemented in the REFPROP 10.0 software [32]. The accuracy of the fluid phase model was verified in a previous study by comparing the calculated and experimentally determined C_3H_8 + H_2O equilibria from T = 235.55 to 399.89 K and from p = 0.7720 to 67.3962 MPa, where an average deviation of ca. 0.2% was observed [35,36].

3.2. Hydrate Phase

The hydrate models reported by van der Waal and Platteeuw [31] and Sloan et al. [22] were used for calculating the fugacity of H_2O in the hydrate phase. The fugacity of H_2O in the filled hydrate cage ($f_{H_2O}^H$) can be express as [22]

$$f_{H_2O}^H = f_{H_2O}^\beta \exp\left(-\frac{\mu_{H_2O}^{\beta-H}}{RT}\right), \tag{3}$$

where $f_{H_2O}^\beta$ is the fugacity of water in the hypothetical empty cage, $\mu_{H_2O}^{\beta-H}$ is the difference between the chemical potential for water in a filled and empty hydrate cages, R is the gas constant, and T represents the temperature.

$f_{H_2O}^\beta$ can be calculated via

$$f_{H_2O}^\beta = \varphi_{H_2O}^\beta p_{H_2O}^\beta \exp \int_{p_{H_2O}^\beta}^{p} \left(\frac{v_{H_2O}^\beta}{RT}\right) dp. \tag{4}$$

In Equation (4), the fugacity coefficient for water in the empty hydrate cavity $\left(\varphi_{H_2O}^\beta\right)$ is assumed to be equal to 1, because the vapour pressure of water in the empty cage ($p_{H_2O}^\beta$) is low, and $v_{H_2O}^\beta$ represents the molar volume of an empty cage.

Sloan et al. [22] also reported an Antoine-like equation for calculating $p_{H_2O}^\beta$ which can be expressed as

$$p_{H_2O}^\beta = \exp\left(a - \frac{b}{T}\right), \tag{5}$$

where a and b are the fitting parameters.

The correlation given by Avlonitis [37] is used for calculating $v^{\beta}_{H_2O}$:

$$v^{\beta}_{H_2O} = v(1 + k_1(T - T) + k_2(T - T)^2 + k_3(T - T)^3), \quad (6)$$

where v denotes the molar volume of the sI hydrate,

k_1, k_2, and k_3 represent the fitted temperature coefficients of the empty sII hydrate, and T is a reference temperature.

$\mu^{\beta-H}_{H_2O}$ is calculated by using the van der Waals and Platteeuw equation given as [31]

$$\frac{\mu^{\beta-H}_{H_2O}}{RT} = \sum_m \overline{v}_m \ln\left(1 - \sum_j \theta_{jm}\right), \quad (7)$$

where $\overline{v}_m$ is the number of cavities of type m per water molecule and θ_{jm} is the fractional cage occupancy. θ_{jm} can be calculated from the Langmuir adsorption equation given as [38]

$$\theta_{jm} = \frac{C_{jm} f_j}{1 + \sum_j C_{jm} f_j}, \quad (8)$$

where f_j denotes the fugacity of pure hydrate former j (C_3H_8) in cavity m ($5^{12}6^4$) and C_{jm} is the Langmuir constant. C_{jm} can be calculated by using a simplified Parrish and Prausnitz [38] correlation which measures the attraction between the gas and water molecules in a hydrate cavity:

$$C_{jm} = \frac{A_{jm}}{T} \exp \frac{B_{jm}}{T}, \quad (9)$$

where A_{jm} and B_{jm} are fitting parameters.

The fugacity of C_3H_8 in Equation (8) was calculated using Lemmon et al. [29] EOS.

Optimization Empty Cage and Langmuir Fitting Parameters

The Langmuir fitted parameters (A_{jm} and B_{jm}) and the empty cage constants (a and b) are guest and hydrate type dependant. The empty cage constants were optimised with the water content measurements reported in this work by minimizing the sum squared difference (SSE) for the fugacities of water in the non-aqueous and hydrate phases. The optimized empty cage constants used in this work were found to be a = 17.43 MPa and b = 5957.51 KMPa^{-1} versus a = 17.33 MPa and b = 6017.60 KMPa^{-1} given by Sloan et al. [22]. Our optimized values are within 1% of the values reported by Sloan et al. [22] with an SSE = 1.95×10^{-7} MPa^2.

The molar volume (22.57 cm^3 mol^{-1}) and thermal expansion coefficients for sII hydrate ($k_1 = 1.9335 \times 10^{-4}$ K^{-1}, $k_2 = 2.1768 \times 10^{-7}$ K^{-2} and $k_3 = -1.4786 \times 10^{-10}$ K^{-3}) given by Alvonitis [37] were used as reported without further optimization. In a previous work, we have optimized the Langmuir fitted parameters given as A_{jm} = 0.1459 KMPa^{-1} and B_{jm} = 3833.66 K with measured three-phase dissociation data [21]. The water content of C_3H_8 in equilibrium with its hydrate at any specified pressure and temperature can be calculated by solving Equation (1) iteratively using the optimized parameters reported in this study.

4. Results and Discussion

4.1. Verification of the TDLAS

The TDLAS analyzer was factory calibrated by the manufacturer for water concentration measurements within different fluids including C_3H_8, and a relative accuracy of 2% was specified; however, at low concentrations we have found a limiting stable standard deviation of 4 ppm H_2O. Thus, we estimate that the 95% confidence interval for this TDLAS should not be better than 12 ppm,

based on signal stability. Using the stability as a limit for accuracy, the TDLAS analyzer was validated with different concentrations of C_3H_8 + H_2O feeds, as shown in Table 1. The average of the differences was similar 12 ppm and no further correction was applied.

Table 1. Difference between the gravimetrically prepared feeds and experimental measured water content for single phase C_3H_8 + H_2O.

$y$$H_2O$ (exp.)/ppm [a]	$y$$H_2O$ (grav.)/ppm	$y$$H_2O$ (grav.) - $y$$H_2O$(exp.)/ppm
92	106 ± 3	14
152	165 ± 8	13
219	223 ± 22	4
251	263 ± 11	12

[a] Reproducibility for water content measurements from triplicate measurements was calculated to be 12 ppm at the 95% confidence interval. This is slightly more conservative than the average 95% confidence in the gravimetric mixtures (shown in the second column).

4.2. Experimental Water Content Measurement

The experimental water contents of C_3H_8 in equilibrium with the hydrate phase and the differences from the thermodynamic model reported in this work are presented in Table 2, while the calculations using this study's model for different isotherms ranging from T = 242 to 276 K are presented in Figure 1.

Table 2. Experimental and calculated water content for liquid C_3H_8 in equilibrium with a hydrate.

p/MPa [a]	T/K [b]	$y$$H_2O$(exp.)/ppm [c]	$y$$H_2O$(calc.)/ppm	$y$$H_2O$(exp.) - $y$$H_2O$(calc.)/ppm
1.081	242.95	10	11	−1
2.484	241.95	10	9	1
9.980	242.86	10	10	0
20.062	243.05	7	10	−3
30.025	242.88	8	10	−2
39.984	243.04	9	10	−1
1.731	253.43	30	24	6
2.319	253.96	34	25	9
10.086	253.02	26	23	3
20.104	253.03	32	22	10
30.148	253.03	33	22	11
40.132	253.03	36	22	14
2.496	263.08	53	49	4
10.106	263.07	45	47	−2
20.142	263.07	49	46	4
30.119	263.07	52	45	7
40.064	263.08	53	44	8
2.545	273.10	88	97	−9
10.088	273.12	84	94	−10
20.132	273.12	84	90	−6
30.107	273.12	83	88	−6
40.077	273.12	82	87	−5
2.553	276.10	110	119	−9
10.005	276.12	105	114	−9
20.004	276.11	100	110	−10
30.037	276.11	98	107	−9
40.010	276.11	94	105	−11

[a] Precision of pressure measurements calculated to be ±0.001 MPa. [b] Precision of temperature measurements was calculated to be ±0.1K. [c] Reproducibility for water content measurements is estimated to be 12 ppm at the 95% confidence interval.

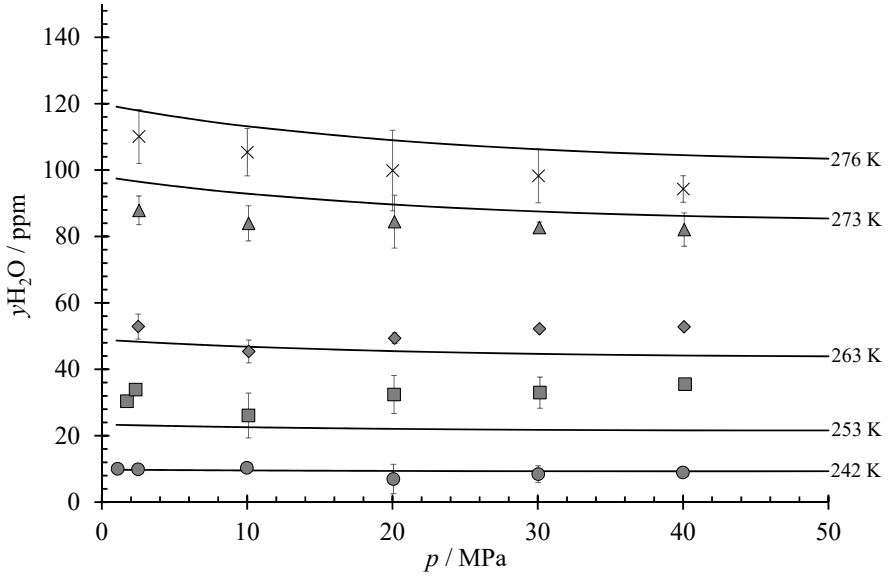

Figure 1. Isotherm plot of water content versus pressure. ———, calculation using the model reported in this study at the different temperatures indicated. Error bars are shown as three times the standard deviation; however, the average 95% confidence is estimated to be 12 ppm.

As shown in Figure 1, the pressure dependence is small for the $C_3H_8(l)$ + hydrate equilibria. This is expected for any equilibria between two relatively incompressible phases and was also noted with the $CO_2(l)$ + hydrate and $H_2S(l)$ + hydrate systems [26,27]. Thus, in place of the more rigorous thermodynamic model reported in this work, a simple non-pressure-dependent semi-empirical equation can be used for rapid calculation:

$$ln\left(y_{H_2O}\right) = \left[(7.86 \pm 0.69) - \left(\frac{4679.29 \pm 179.28}{T/K}\right)\right]. \quad (10)$$

A parity plot between the experimental data and calculated values using our more rigorous thermodynamic model is presented in Figure 2. All calculated and experimental values reported in this work agree with less difference than the stated 12 ppm precision limit. The average difference from this study's thermodynamic model and semi-empirical correlation, equilibrium conditions, pressure, and corresponding temperature ranges are presented in Table 3.

Table 3. Measured water content data and their corresponding average difference and standard deviation from this study's thermodynamic model for C_3H_8 (l)-H systems.

T Ranges/K	p Ranges/MPa	Number of Data Points	Average Difference from this Study's Thermodynamic Model (σ_{AD}) /ppm	Average Difference from this Study's Semi-Empirical Correlation (σ_{AD})/ppm	Reference
246.7–276.5	0.772	9	24.8 (14.8)	27.4 (17.4)	Sloan et al. [22]
211.15–270.85	0.86	6	2.4 (9.7)	−2.6 (2.3)	Song et al. [23]
235.65–276.15	1.097	7	−6.0 (2.9)	−5.0 (4.4)	Song and Kobayashi [24]
246.66–276.4	0.772–3.45	11	24.9 (13.6)	27.2 (16.1)	Sloan et al. [25]
241.95–276.11	1.081–40.064	27	0.7 (7.3)	−1.0 (8.4)	This study

Sloan et al. [22], Song et al. [23], and Song and Kobayashi [24] all reported water content data for isobars less than 1.1 MPa at different temperatures ranging from 211 to 276 K. As shown in Table 3, the lowest average difference to the thermodynamic model and semi-empirical correlation reported in this study was observed in the data reported by Song et al. [23] and Song and Kobayashi [24]. The highest average difference was observed in the data reported by Sloan et al [25]. Using the same type of experimental setup, Sloan et al. [22] re-examined their previous measurements with some modelling

effort for pressure p = 0.772 MPa at different temperatures. The data set reported are similar to the earlier reported set where a comparable average difference was observed.

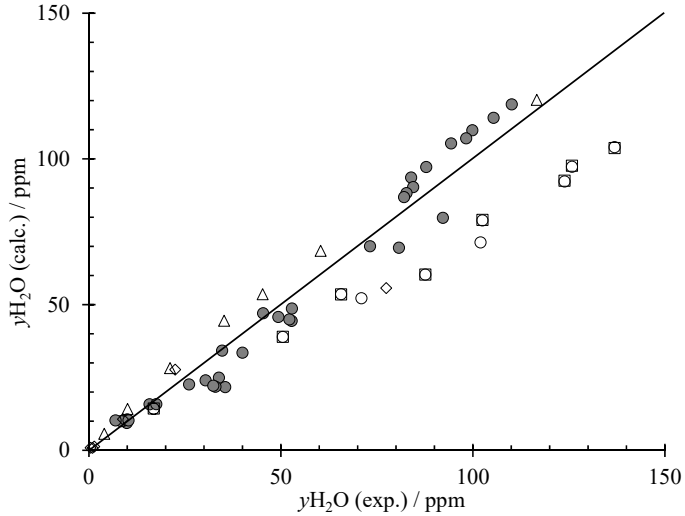

Figure 2. Parity plot of the water content data for C_3H_8 in the presence of a hydrate phase. •, this study measurement; □, Sloan et al. [22]; ◊, Song et al. [23]; Δ, Song and Kobayashi [24]; ○, Sloan et al. [25]; and straight line is a perfect correlation.

4.3. Comparison of Three Phase Hydrate Dissociation Data to This Study's Model

A summary of all the dissociation conditions in the presence of water reported in the literature along the Lw–H–C_3H_8(g) and Lw–H–C_3H_8(l) phase boundaries, in addition to water content conditions of this study are presented in Figure 3.

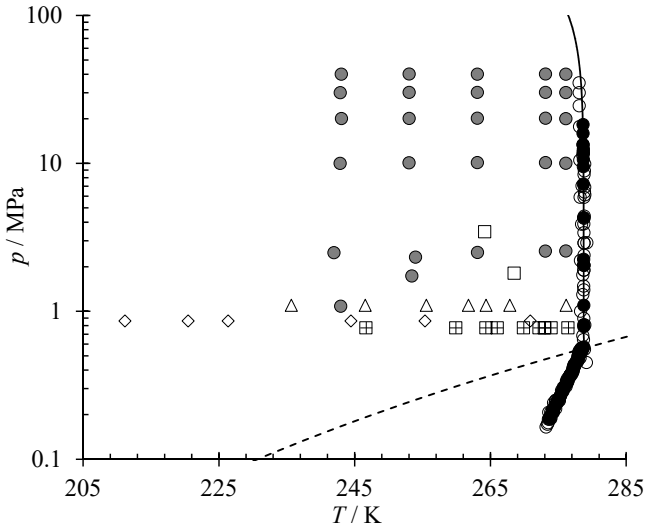

Figure 3. Summary of experimental C_3H_8 dissociation data along the Lw–H–C_3H_8(g) and Lw–H–C_3H_8(l) phase boundaries, and the measured water content conditions of this work. Solid black line represents calculated values using the three phase model reported by Adeniyi et al. [21], broken line is the calculated vapour pressure of pure C_3H_8 using Lemmon et al. equation equations-of-state (EOS) [29], filled black circle represents Adeniyi et al. [21] measurements, open circle represents other literature measurements along the Lw–H–C_3H_8(g) and Lw–H–C_3H_8(l) phase boundaries [5–20], and grey circle is the measured conditions for C_3H_8 in equilibrium with a hydrate of this study. □, Sloan et al. [22]; ◊, Song et al. [23]; Δ, Song and Kobayashi [24]; and +, Sloan et al. [25].

In our previous study [21], we measured the dissociation condition along the Lw–H–C_3H_8(g) and Lw–H–C_3H_8(l) locus using two different purities of C_3H_8 (99.5 mol% and 99.999 mol%). Moreover, we modelled the measurements using the Holder et al. [39] and van der Waal and Platteeuw [31] equations for the hydrate phase fugacity calculation, as well as the Lemmon et al. [29] and Feistel and Wagner [34] EOSs coupled with the mixing parameters of Kunz and Wagner [30] for the fluid phase fugacity calculation. The results obtained from the thermodynamic model (shown in Figure 3) were compared to the experimental measurements in the literature [5–20] where an average deviation of 0.25 K was observed [21]. Despite the Langmuir adsorption showing nearly complete cage occupancy (from 0.996 to 0.99999 fractional occupancy) with a single former, optimization of Langmuir adsorption parameters has been a robust method for the three phase loci for several systems.

This study's thermodynamic model also was used to calculate the three phase loci [Lw–H–C_3H_8(g) and Lw–H–C_3H_8(l)]. As discussed, our previously reported Langmuir fitted parameters for the three phase loci [21] together with the optimised empty cage constant using the measured water content of this study was used in this model. Generally, the calculated values showed a much larger deviation (>5 K) compared to the available literature [5–20]. The model reported by Adeniyi et al. [21] is recommended for the three phase loci calculation and can be used for establishing the upper limit for C_3H_8-hydrate system. We note that optimization of the empty cage and Langmuir parameters did not results in a parameter set which could reasonably reproduce both water content and the three phase loci. With the sI CO_2 system, we were able to iteratively optimize all coefficients by using water content for the empty cage parameters and occupancy (Langmuir) for the three phase loci. This same approach was not successful for the sII C_3H_8 system or the sI H_2S system. Future efforts may be successful by changing the equation forms for the empty cage or the interaction potential. Thus, for the three-phase or two-phase calculations involving C_3H_8, different models are currently recommended for each type of phase behaviour, versus the preference for a single hydrate model that uses same optimized parameters for both three phase and water content calculation. This was also the case for our H_2S(l) + hydrate modelling efforts [27].

5. Conclusions

New experimental data for the water content of C_3H_8(l) in the presence of a sII hydrate phase are reported and modelled. The reduced Helmholtz EOSs for C_3H_8 [29] and H_2O [28,34] with the mixing parameters of Kunz and Wagner [30] were employed to model the non-hydrate phase, while the van der Waals and Platteuw [31] and Sloan et al. [22] equations are used for the hydrate phase. In the model reported in this study, only the empty cages parameters were optimised using the measured water content data of this study.

Using these optimized parameters, the calculations from the model were compared to few available C_3H_8 water content data in equilibrium with a hydrate, where a relatively good agreement (average difference of less than 12 ppm) was observed. The same model was used to calculate the dissociation conditions for the three phase loci where a large deviation of ca. 7 K was observed for the Lw–H–C_3H_8(g) and Lw–H–C_3H_8(l) phase boundaries. Thus, the previous parameters reported by Adeniyi et al. [21] are recommended for the three phase loci calculation. These new water content measurements and model parameters will be useful for estimating how much dehydration is necessary to avoid hydrate formation during C_3H_8 transportation and processing.

Author Contributions: Research conceptualization, methodology, software, validation, investigation, data curation, writing—original draft preparation, visualization, K.I.A., C.E.D. and R.A.M.; formal analysis, resources, writing—review and editing, K.I.A., C.E.D. and R.A.M.; supervision, project administration, funding acquisition, R.A.M. All authors have read and agreed to the published version of the manuscript.

Funding: This research was funded by the Natural Sciences and Engineering Council of Canada (NSERC) and Alberta Sulphur Research Ltd. (ASRL) through the NSERC ASRL Industrial Research Chair in Applied Sulfur Chemistry.

Acknowledgments: The authors are grateful for funding through the NSERC ASRL Industrial Research Chair in Applied Sulfur Chemistry and the sponsoring companies of Alberta Sulphur Research Ltd.

Conflicts of Interest: The authors declare no conflict of interest.

References

1. Kidnay, A.J.; Parrish, W.; Parrish, W.R. *Fundamentals of Natural Gas Processing*; CRC Press: Boca Raton, FL, USA, 2006; Volume 2.
2. Sloan, E.D.; Koh, C.A.; Sum, A.; Ballard, A.L.; Creek, J.L.; Eaton, M.; Lachance, J.; McMullen, N.; Palermo, T.; Shoup, G.; et al. *Natural Gas Hydrates in Flow Assurance*; Gulf Professional Publishing (Elsevier): Oxford, UK, 2010; ISBN 978-1-85617-945-4.
3. Carroll, J. *Natural Gas Hydrates, a Guide for Engineers*, 2nd ed.; Gulf Professional Publishing: Burlington, MA, USA, 2009.
4. Ward, Z.T.; Marriott, R.A.; Sum, A.K.; Sloan, E.D.; Koh, C.A. Equilibrium Data of Gas Hydrates containing Methane, Propane, and Hydrogen Sulfide. *J. Chem. Eng. Data* **2015**, *60*, 424–428. [CrossRef]
5. Reamer, H.H.; Selleck, F.T.; Sage, B.H. Some Properties of Mixed Paraffinic and Olefinic Hydrates. *J. Pet. Technol.* **1952**, *4*, 197–202. [CrossRef]
6. Tumba, K.; Babaee, S.; Naidoo, P.; Mohammadi, A.H.; Ramjugernath, D. Phase Equilibria of Clathrate Hydrates of Ethyne + Propane. *J. Chem. Eng. Data* **2014**, *59*, 2914–2919. [CrossRef]
7. Patil, S.L. Measurement of Multiphase Gas Hydrate Phase Equilibria: Effect of Inhibitors and Heavier Hydrocarbon Components. Master's Thesis, University of Alaska, Anchorage, AL, USA, 1987.
8. Robinson, D.; Metha, B. Hydrates in the Propane–Carbon dioxide–Water System. *J. Can. Pet. Technol.* **1971**, *10*, 642–644. [CrossRef]
9. Englezos, P.; Ngan, Y.T. Incipient Equilibrium Data for Propane Hydrate Formation in Aqueous Solutions of NaCl, KCl, and $CaC1_2$. *J. Chem. Eng. Data* **1993**, *38*, 250–253. [CrossRef]
10. Verma, V.K. Gas Hydrates from Liquid Hydrocarbon-Water Systems. Ph.D. Thesis, University of Michigan, Ann Arbor, MI, USA, 1974.
11. Kubota, H.; Shimizu, K.; Tanaka, Y.; Makita, T. Thermodynamic Properties of R13 ($CClF_3$), R23 (CHF_3), R152a ($C_2H_4F_2$) and Propane Hydrates for Desalination of Seawater. *J. Chem. Eng. Jpn.* **1984**, *17*, 423–429. [CrossRef]
12. Deaton, W.; Frost, J.E. *Gas Hydrates and Their Relation to the Operation of Natural-Gas Pipe Lines*; U.S. Bureau of Mines, Monograph: New York, NY, USA, 1946; Volume 8.
13. Thakore, J.L.; Holder, G.D. Solid Vapor Azeotropes in Hydrate-Forming Systems. *Ind. Eng. Chem. Res.* **1987**, *26*, 462–469. [CrossRef]
14. Den Heuvel, M.M.M.; Peters, C.J.; de Swaan Arons, J. Gas Hydrate Phase Equilibria for Propane in the Presence of Additive Components. *Fluid Phase Equilibria* **2002**, *193*, 245–259. [CrossRef]
15. Nixdorf, J.; Oellrich, L.R. Experimental Determination of Hydrate Equilibrium Conditions for Pure Gases, Binary and Ternary Mixtures and Natural gases. *Fluid Phase Equilibria* **1997**, *139*, 325–333. [CrossRef]
16. Maekawa, T. Equilibrium Conditions of Propane Hydrates in aqueous Solutions of Alcohols, Glycols, and Glycerol. *J. Chem. Eng. Data* **2008**, *53*, 2838–2843. [CrossRef]
17. Miller, B.; Strong, E.R. Hydrate Storage of Natural Gas. *Am. Gas Assoc.* **1946**, *28*, 63–67.
18. Kamath, V.A. Study of Heat Transfer Characteristics during Dissociation of Gas Hydrates. Ph.D. Thesis, University of Pittsburgh, Pittsburgh, PA, USA, 1984.
19. Makogon, Y.F. Liquid Propane + Water Phase Equilibria at Hydrate Conditions. *J. Chem. Eng. Data* **2003**, *48*, 347–350. [CrossRef]
20. Wilcox, W.; Carson, D.; Katz, L. Natural Gas Hydrates. *Ind. Eng. Chem.* **1941**, *33*, 662–665. [CrossRef]
21. Adeniyi, K.I.; Deering, C.E.; Marriott, R.A. Hydrate Decomposition Conditions for Liquid Water and Propane. *J. Chem. Eng. Data* **2017**, *62*, 2222–2229. [CrossRef]
22. Sloan, E.D.; Sparks, K.A.; Johnson, J.J. Two-phase Liquid Hydrocarbon- Hydrate Equilibrium for Ethane and Propane. *Ind. Eng. Chem. Res.* **1987**, *26*, 1173–1179. [CrossRef]
23. Song, K.Y.; Yarrison, M.; Chapman, W. Experimental Low-Temperature Water Content in Gaseous Methane, Liquid Ethane, and Liquid Propane in Equilibrium with Hydrate at Cryogenic Conditions. *Fluid Phase Equilibria* **2004**, *224*, 271–277. [CrossRef]
24. Song, K.Y.; Kobayashi, R. The Water Content of Ethane, Propane and their Mixtures in Equilibrium with Liquid Water or Hydrates. *Fluid Phase Equilibria* **1994**, *95*, 281–298. [CrossRef]

25. Sloan, E.D.; Bourrie, M.S.; Sparks, K.A.; Johnson, J.J. An Experimental Method for the Measurement of Two-Phase Liquid Hydrocarbon-Hydrate Equilibrium. *Fluid Phase Equilibria* **1986**, *29*, 233–240. [CrossRef]
26. Adeniyi, K.I.; Deering, C.E.; Grynia, E.; Marriott, R.A. Water Content and Hydrate Dissociation Conditions for Carbon dioxide rich Fluid. *Int. J. Greenh. Gas Control* **2020**, *101*, 103139. [CrossRef]
27. Adeniyi, K.I.; Bernard, F.; Deering, C.E.; Marriott, R.A. Water Content of Liquid H_2S in Equilibrium with the Hydrate Phase. *Fluid Phase Equilibria* **2020**, *529*, 112865. [CrossRef]
28. Wagner, W.; Pruß, A. The IAPWS Formulation 1995 for the Thermodynamic Properties of Ordinary Water Substance for General and Scientific Use. *J. Phys. Chem. Ref. Data* **2002**, *31*, 387–535. [CrossRef]
29. Lemmon, E.W.; McLinden, M.O.; Wagner, W. Thermodynamic Properties of Propane. III. A Reference Equation of State for Temperatures from the Melting line to 650 K and Pressures up to 1000 MPa. *J. Chem. Eng. Data* **2009**, *54*, 3141–3180. [CrossRef]
30. Kunz, O.; Wagner, W. The GERG-2008 Wide-range Equation of State for Natural Gases and other Mixtures: An Expansion of GERG-2004. *J. Chem. Eng. Data* **2012**, *57*, 3032–3091. [CrossRef]
31. Van der Waals, J.H.; Platteeuw, J.C. Clathrate Solutions. *Adv. Chem. Phys.* **1959**, *2*, 1–57.
32. Lemmon, E.W.; Bell, I.H.; Huber, M.L.; McLinden, M.O. *NIST Standard Reference Database 23: Reference Fluid Thermodynamic and Transport Properties-REFPROP, Version 10.0*; National Institute of Standards and Technology: Gaithersburg, MD, USA, 2013.
33. Preston-Thomas, H. The International Temperature Scale of 1990 (ITS 90). *Metrologia* **1990**, *107*, 186–194.
34. Feistel, R.; Wagner, W. A new Equation of State for H_2O Ice Ih. *J. Phys. Chem. Ref. Data* **2006**, *35*, 1021–1047. [CrossRef]
35. Adeniyi, K.I. Thermodynamic Formation Conditions of Propane Hydrate in Equilibrium with Liquid Water. Master's Thesis, University of Calgary, Calgary, AB, USA, 2016.
36. Deering, C.E.; Carefoot, S.K.; Bernard, F.; Giri, B.R.; Marriott, R.A. Effect of Gas Gravity, H_2S, and Salinity on the Water Content of Natural Gas: Part I, Effect on Gas Gravity. GPA Research Project No. 074-1; GPA Midstream Association (GPA Midstream): Tulsa, OK, USA, 2017.
37. Avlonitis, D. The Determination of Kihara Potential Parameters from Gas Hydrate Data. *Chem. Eng. Sci.* **1994**, *49*, 1161–1173. [CrossRef]
38. Parrish, W.R.; Prausnitz, J.M. Dissociation pressures of gas hydrates formed by gas mixtures. *Ind. Eng. Chem. Process Des. Dev.* **1972**, *11*, 26–35. [CrossRef]
39. Holder, G.D.; Corbin, G.; Papadopoulos, K.D. Thermodynamic and Molecular Properties of Gas Hydrates from Mixtures containing Methane, Argon, and Krypton. *Ind. Eng. Chem. Fundam.* **1980**, *19*, 282–286. [CrossRef]